Space Sci Rev (2011) 158: 69–89
DOI 10.1007/s11214-010-9715-2

Interplanetary Origin of Intense, Superintense and Extreme Geomagnetic Storms

Walter D. Gonzalez · Ezequiel Echer · Bruce T. Tsurutani · Alicia L. Clúa de Gonzalez · Alisson Dal Lago

Received: 26 May 2010 / Accepted: 20 October 2010 / Published online: 29 March 2011

Abstract We present a review on the interplanetary causes of intense geomagnetic storms ($Dst \leq -100$ nT), that occurred during solar cycle 23 (1997–2005). It was reported that the most common interplanetary structures leading to the development of intense storms were: magnetic clouds, sheath fields, sheath fields followed by a magnetic cloud and corotating interaction regions at the leading fronts of high speed streams. However, the relative importance of each of those driving structures has been shown to vary with the solar cycle phase. Superintense storms ($Dst \leq -250$ nT) have been also studied in more detail for solar cycle 23, confirming initial studies done about their main interplanetary causes. The storms are associated with magnetic clouds and sheath fields following interplanetary shocks, although they frequently involve consecutive and complex ICME structures. Concerning extreme storms ($Dst \leq -400$ nT), due to the poor statistics of their occurrence during the space era, only some indications about their main interplanetary causes are known. For the most extreme events, we review the Carrington event and also discuss the distribution of historical and space era extreme events in the context of the sunspot and Gleissberg solar activity cycles, highlighting a discussion about the eventual occurrence of more Carrington-type storms.

Keywords Intense geomagnetic storms · Geomagnetic activity · Extreme geomagnetic storms

1 Introduction

Intense geomagnetic storms are those for which the storm Dst index achieves values ≤ -100 nT (Gonzalez et al. 1994). Superstorms are those events for which Dst obtains values less than -250 nT (e.g. Tsurutani et al. 1992a; Gonzalez et al. 2002;

W.D. Gonzalez (✉) · E. Echer · A.L. Clúa de Gonzalez · A. Dal Lago
National Institute of Space Research, Sao Jose dos Campos, SP, Brazil
e-mail: gonzalez@dge.inpe.br

B.T. Tsurutani
Jet Propulsion Laboratory, California Institute of Technology, Pasadena, CA, USA

Echer et al. 2008b) and extreme storms are those for which the Dst values become less than -400 nT (Gonzalez et al. 2010). During the space era (since 1957) there have been only five extreme storms, as seen in Table 2, and during the last solar cycle (# 23) there has been only one extreme storm that occurred on November 20, 2003.

Gonzalez and Tsurutani (1987) and Tsurutani et al. (1988) studied the interplanetary causes of intense geomagnetic storms ($Dst \leq -100$ nT) for the peak interval of the maximum phase of solar cycle 21 and found that approximately half of the storms were associated with magnetic clouds and half with sheath field regions behind interplanetary shocks. Later, several authors have studied the geoeffectiveness of magnetic clouds for longer time intervals (Gosling et al. 1991; Echer et al. 2005) and of other interplanetary structures for several levels of the intensity of magnetic storms, also involving superstorms (Gonzalez et al. 1994, 1999, 2002; Huttunen et al. 2002; Echer et al. 2004; Srivastava 2005; Zhang et al. 2006; Richardson et al. 2006; Alves et al. 2006; Gonzalez et al. 2007; Echer et al. 2008a, 2008b).

Tsurutani et al. (2003) reported extreme historical storms, for which the Carrington storm of September 2, 1859 was the most intense. Whereas during the space era the most extreme recorded storm was that of March 13, 1989, with a peak Dst index of nearly -600 nT, the historical storms listed on Table 1 of Tsurutani et al. (2003) had associated peak-ring current intensity values < -600 nT. We can not be certain about the associated peak Dst values for the historical storms since the Dst index started to be constructed and published only since 1957. However, judging from the peak ΔH-incursion values observed in the low latitude magnetograms of the historical storms (see also Lakhina et al. 2005), one can claim that the associated Dst values would have been at times almost as large as the proper ΔH-incursions (Echer and Gonzalez 2007). Gonzalez et al. (2010) have extended the study of extreme storms with respect to their association with the sunspot and Gleissberg cycles of solar activity and have discussed the apparent occurrence tendency of Carrington-type extreme storms during the Gleissberg cycles.

In Sect. 2 of this review we summarize some of the main findings concerning the interplanetary origin of intense storms. In Sect. 3, we present some of the recently reported interplanetary structures associated with superintense storms, mainly for solar cycle 23. Finally, in Sect. 4, some interplanetary and magnetospheric features associated with extreme storms are described.

2 Intense Storms

Gonzalez et al. (2007) and Echer et al. (2008b) investigated the interplanetary causes of 87 intense storms ($Dst \leq -100$ nT) during solar cycle 23. For identification, they followed the nomenclature and definitions given by Burlaga et al. (1987), Tsurutani et al. (1988, 1995), Gonzalez et al. (1999), Balogh et al. (1999). Table 1 gives the yearly distribution of those intense storms according to their interplanetary causes. "CIR" stands for corotating interaction region (associated with a high speed stream), "MC" for a magnetic cloud (a common type of a ICME driver), "Sh + MC" for a sheath B_s (B_z southward) field followed by a magnetic cloud, "SBC" for a sector boundary crossing, "S compr MC" for a magnetic cloud compressed by a shock, and Complex for a case in which none of the other cases were identified.

The category of sheath fields corresponds to B_s fields in the sheath region that follow an interplanetary shock without any other B_s structure behind the sheath region that could also be responsible for the development of the storm' s main phase. In the category of Sh + MC, a magnetic cloud (also with a B_s field) following the sheath region was observed to be partly

Table 1 Interplanetary structures that caused intense geomagnetic storms per year during cycle 23

Year/IP structure[a]	CIR	MC	Sh + MC	Sh	Slow MC	ICME	Sh + ICME	ICME + SBC	Sh + SBC	SC MC	ICME + CIR	Complex	Alfven waves?
1997	–	1	2	1	1	–	–	–	–	–	–	–	–
1998	1	2	1	2	–	2	–	1	1	1	–	–	–
1999	–	2	–	1	–	1	–	–	–	–	1	–	–
2000	1	4	3	1	–	1	–	–	–	–	–	1	–
2001	–	2	2	6	1	1	1	–	–	–	–	–	–
2002	4	2	2	4	1	–	1	–	–	–	–	–	–
2003	2	2	–	2	–	–	–	–	–	–	–	1	–
2004	1	3	2	2	–	2	–	–	–	–	–	–	–
2005	2	3	–	2	2	1	–	–	–	–	–	–	1
Total[b]	11	21	12	21	5	8	2	1	1	1	1	2	1

[a]Abbreviations are CIR, corotating interaction region; MC, magnetic cloud; Sh + MC, sheath field followed by a magnetic cloud; Sh, sheath field; ICME, interplanetary coronal mass ejection; SBC, sector boundary crossing; SC MC, shock compressed magnetic cloud

[b]The total number of storms is 87

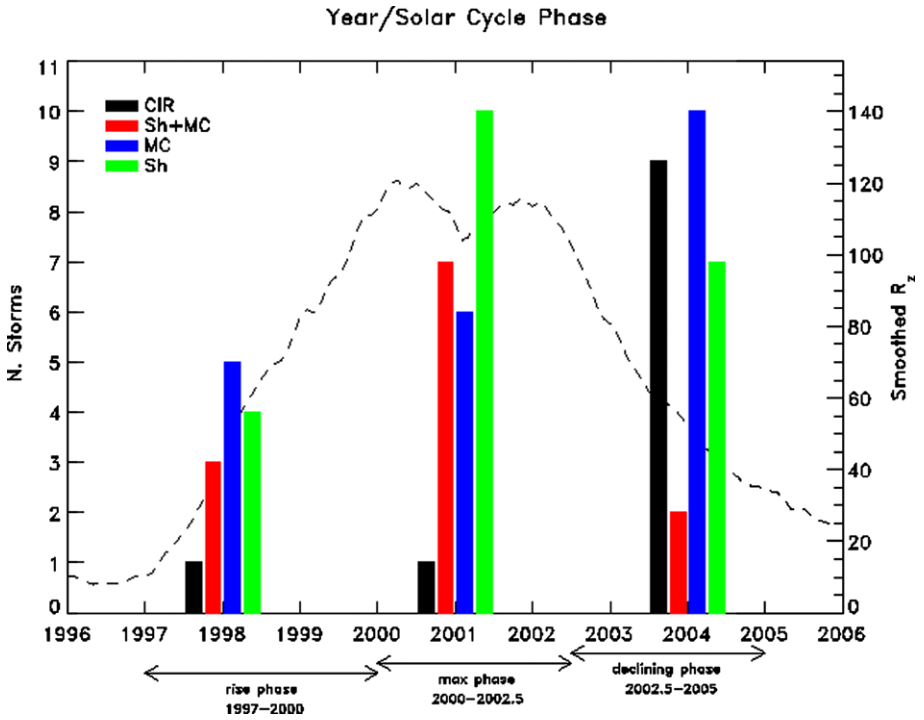

Fig. 1 Distribution of the four main interplanetary structures causing intense magnetic storms according to the phase of the solar cycle 23

responsible for the development of the storm. The category of "ICMEs" (interplanetary coronal mass ejections) corresponds to several types of structures (e.g., Tsurutani et al. 1988; Gonzalez et al. 1999) that are not magnetic clouds, namely that do not have the typical signatures for magnetic clouds (Burlaga et al. 1987).

One can see in Table 1 that the four most common interplanetary structures responsible for the development of intense storms were MC, Sh + MC, Sh, and CIR, with a total number of 21, 12, 21 and 11 cases, respectively. Thus, among these, MCs and Sheath fields were the most common driving structures. From Table 1, one can compute that the four most common structures represent a total of 75% of the interplanetary structures causing intense storms during solar cycle 23, with MCs causing 24%, sheath fields 24%, sheath + MCs 14% and CIRs 13% of the storms. Although in Table 1 the category of ICMEs has a relatively substantial contribution (8 cases), they were not selected among the top driving structures because they correspond to several types of B_s structures that appear to be driving an interplanetary shock and, therefore, do not belong to a single structure, as the selected top four structures do.

Gonzalez et al. (2007) studied the distribution of the four main interplanetary causes according to the selected solar cycle phases *R* (rising), *M* (maximum) and *D* (declining), and represented it with the histograms of Fig. 1, in which the blue color stands for MCs, green for Sheath fields, red for Sh + MC and black for CIRs. For the rising phase, one can observe that the largest fraction of storms are due to magnetic clouds, second to sheath fields and third to the combination of sheath fields followed by magnetic clouds (CIRs represent only a minor contribution to this phase). For the maximum phase, the largest fraction of

storms are associated with sheath fields, second with sheath fields followed by magnetic clouds and third with magnetic clouds (again for this phase, CIRs represent only a minor contribution). For the declining phase, more storms are related to magnetic clouds, second to CIRs and third to sheath fields (a minor contribution is due to sheath fields followed by magnetic clouds).

Figure 2 is an example of an intense storm that occurred in July 26–29, 2004, for which the main phase development was associated with B_s fields in the sheath and MC regions of an ICME. This is also an example of a two-step main phase storm (Kamide et al. 1998). Although most of the intense storms studied for the solar cycle 23 by Gonzalez et al. (2007) and by Echer et al. (2008b) were found to have a single interplanetary cause, e.g., only one ICME, associated with the development of the main phase, Zhang et al. (2007), Yermolaev and Yermolaev (2008), and Cid et al. (2008) believe that several intense storms of cycle 23 were associated with complex interplanetary structures, involving two or more ICMEs. In fact, some of the intense storms have been later associated with such a complex interplanetary origin, especially the most intense ones (e.g. Gonzalez et al. 2008; Tsurutani et al. 2008), as discussed in the following section.

Figure 3 shows histograms for the occurrence distribution of the peak values of the interplanetary magnetic field and electric field parameters B_s and E_y for the intense storms of cycle 23. One can see in these histograms that the peak B_s values are mostly distributed between 10 and 20 nT, with the corresponding peak E_y values distributed mostly between 5 and 10 mV/m. The lower limits of these intervals correspond to the criteria values for intense storms given by Gonzalez and Tsurutani (1987).

Figure 4 shows correlations between peak values of some interplanetary parameters with peak Dst for the intense storms of cycle 23 (Echer et al. 2008a). One can see that the parameters that correlate better are the B_s and E_y fields. However, for more intense storms, it will be noted that the duration of B_s, and especially of E_y, together with their peak values (namely their time integrals), appear to have better correlations with peak Dst. In this figure one can also see that B_p, peak value of the IMF, has a large correlation with peak Dst, almost as large as that between peak Dst and peak B_s. This may be due to the fact that, for intense storms, peak B_s is a substantial fraction of peak B, with an average value of 70%, as discussed by Gonzalez et al. (2004). Also peak B_y shows a moderate correlation with peak Dst in this figure, which may indicate that magnetopause reconnection is influenced by large values of B_y, leading to a tilted reconnection line (e.g. Gonzalez and Mozer 1974).

3 Superintense Storms

Although there is no extensive study of superstorms for the whole space era, some of the main reported results are mentioned below. Table 2 shows the list of superstorms of the space era, with their dates of occurrence and peak Dst values.

Figure 5a shows the solar cycle distribution of the yearly number of superstorms of Table 2. We can see from this figure that superstorms occurred during all phases of the solar cycle, although with a higher tendency around solar maximum and at the early descending phase of the cycle. Figure 5b shows the average solar cycle distribution of that shown in Fig. 5a. This figure clearly shows a dual-peak distribution of superintense storms, as it was also found before for intense storms (Gonzalez et al. 1990a). The first peak occurs at solar maximum and the second one at the descending part of the solar cycle.

Figure 5c shows the seasonal distribution of superstorms for the space era (Gonzalez et al. 2010), in which we can see the equinoctial peaks and also some indication of the July peak, initially found for the distribution of intense storms (Clúa de Gonzalez et al. 2001).

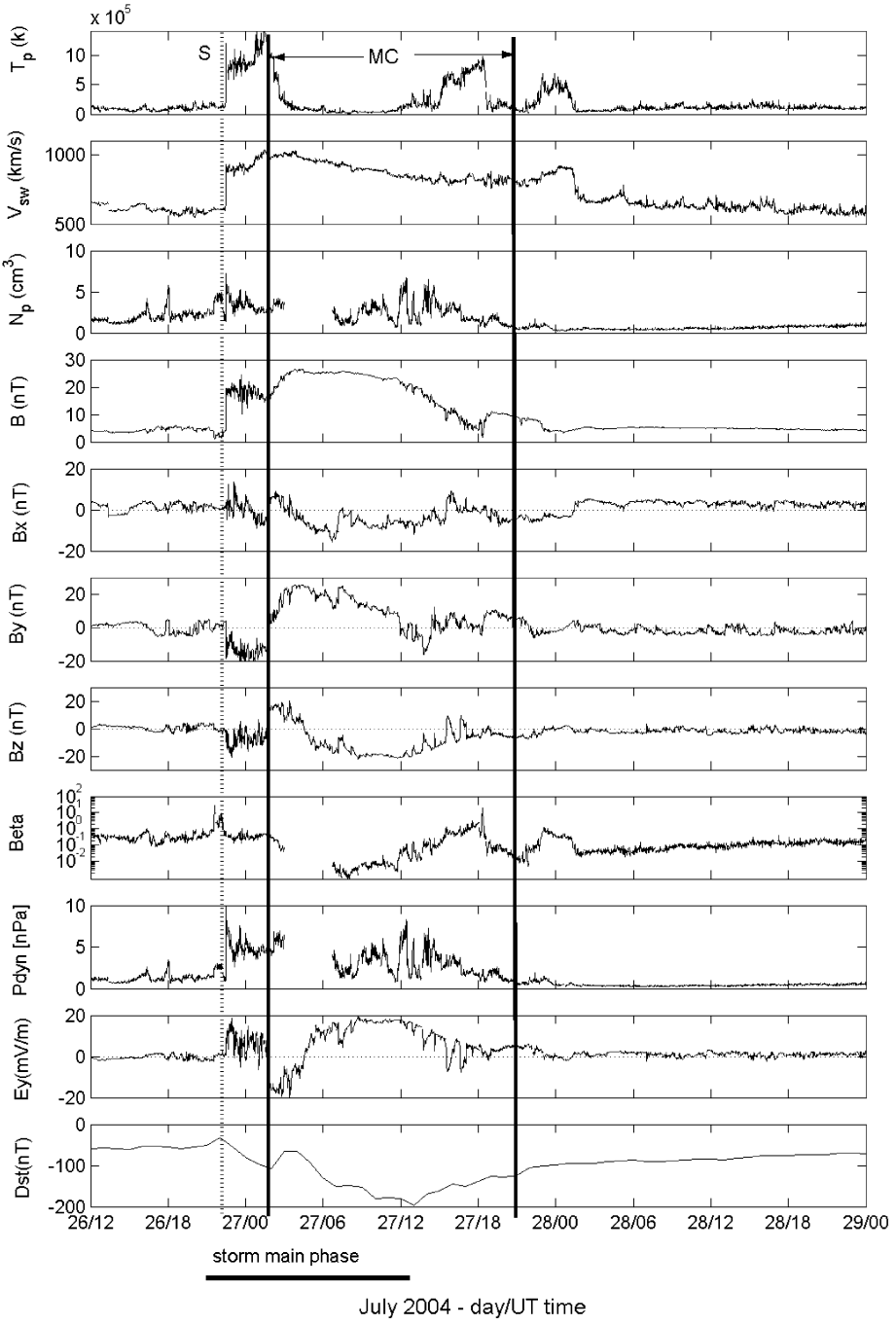

Fig. 2 Example of an intense magnetic storm caused by MC + Sheath fields for July, 26–29, 2004. The figure shows interplanetary parameters measured by the *ACE* satellite and the *Dst* index. Panels are, *from top to bottom*, solar wind proton temperature (T_p), solar wind speed (V_{sw}), proton density (N_p), magnetic field magnitude (B), and components (B_x, B_y, B_z) in GSM, plasma beta parameter (*Beta*), dynamic pressure (P_{dyn}), dawn-dusk electric field component (E_y), and *Dst* index

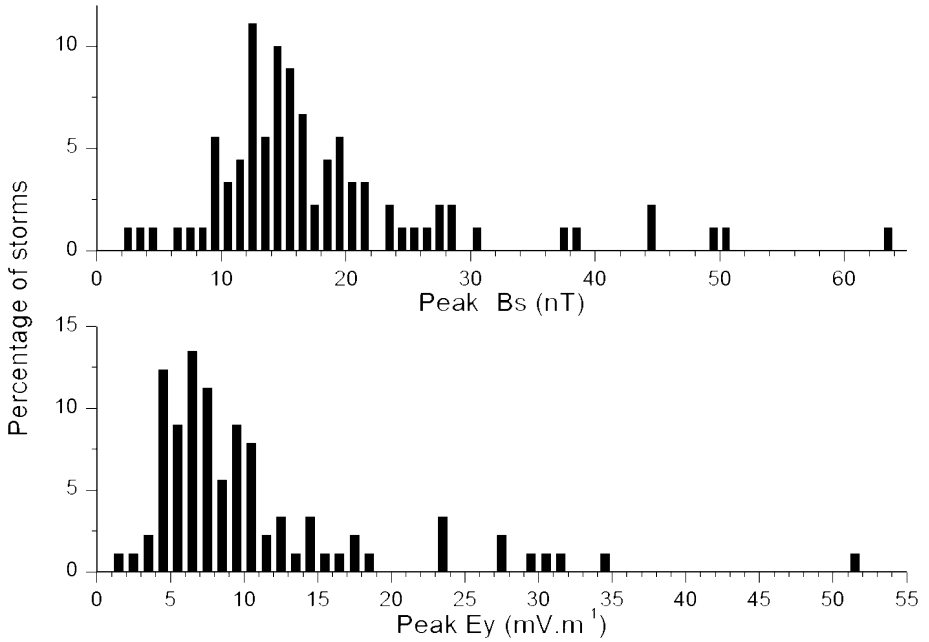

Fig. 3 Peak B_s and peak E_y occurrence histograms for intense storms of solar cycle 23

Table 3 shows the results of a limited study about the solar wind parameters associated with the superintense storms of the space era, for which solar wind data were available (marked with an asterisk in Table 2). We show the average peak values of Dst of the solar wind speed, of the IMF intensity, of the southward component of the IMF (B_s) and of the interplanetary electric field (E_y), together with their corresponding standard deviations and median values. As expected for superstorms, the solar wind speed, density and dynamic pressure and the IMF attain relatively large values, of about 800 km/s, 25 cm^{-3}, 26 nPa and 42 nT, respectively. Also the B_s and E_y parameters attained large values, of -34 nT and 24 mV/m, respectively. The average time delay between peak E_y and peak B_s with peak Dst was of about 1.5 hours (because no time correctionshift between L_1 and the Bow shock was applied for the solar wind data measured by $ISEE-3$, $WIND$ and ACE satellites). The implication of these large interplanetary values for the occurrence of superstorms is discussed below.

Echer et al. (2008a) studied the superstorms ($Dst \leq -250$ nT) that occurred during solar cycle 23. Among their results, they concluded that the main interplanetary causes of those storms were large and sustained B_s fields in magnetic clouds, sheath regions of ICMEs and their combined structures. Similar results were reported before by Tsurutani et al. (1992a) also for superintense storms, studied for the interval of 1971 to 1986. However, for the category of superstorms, the percentage of storms associated with more than one ICME was notably larger than for intense storms (e.g. Cid et al. 2008; Tsurutani et al. 2008). Figure 6 is an example of a superstorm (March 31, 2001), in which the main phase becomes intensified as a result of a combination of two interacting ICMEs. The second ICME compresses the first ICME and, as a result, the southward part of the B_z field in the first magnetic cloud becomes more intense, thus leading to a more intense storm (see also Dal Lago et al. 2004). Similarly, Tsurutani et al. (2008) studied the superstorm of

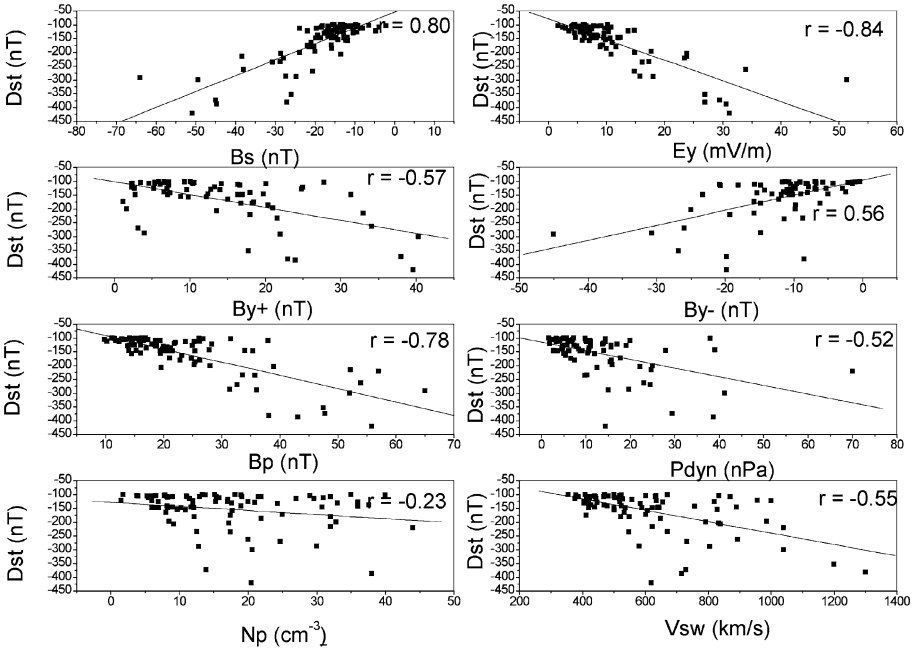

Fig. 4 Correlation between peak Dst and peak interplanetary parameters: B_s (negative B_z), E_y (Y-component of the solar wind electric field), B_y+ (dawn to dusk values of the B_y component of the IMF), B_y, B_p (peak value of the IMF), P_{dyn} (dynamic pressure of the solar wind), N_p (peak value of the solar wind density), and V_{sw} (solar wind speed), for the intense storms of solar cycle 23

November 7–8, 2004, in which several interplanetary features from a complex set of ICMEs played a role in the development of the main phase of this storm. Among those features, Tsurutani et al. (2008) discussed the presence of fast forward shocks, interplanetary directional discontinuities and reverse waves besides a magnetic cloud. Echer et al. (2008a) also showed correlations between peak Dst and peak values of V_{sw}, B, B_s, E_y and the time integral of E_y (during the main phase). They found that the time integral of E_y, rather than peak B_s or peak E_y, had the best correlation with peak Dst. A similar result was also obtained by Srivastava (2005).

4 Extreme Storms

During the space era there were only five extreme storms ($Dst \leq -400$ nT), as seen in Table 2. They occurred on September 13, 1957, February 11, 1958, July 15, 1958, March 13, 1989, and November 20, 2003.

Figure 7 shows the interplanetary data for the extreme storm of November 2003, which is the only extreme storm with a full set of measured interplanetary parameters. One can see from this figure that this extreme storm was caused by the magnetic cloud of a single-well behaved ICME. The five extreme storms of the space era had peak Dst values mostly near -400 nT, with only the storm of March 1989 having a substantially larger peak Dst (≈ -600 nT).

Table 2 List of superstorms (*Dst* 250 nT) during the space era. The events with asterisk are those for which solar wind measurements were available

Date	*Dst*	Date	*Dst*
1957/01/21	−250	1989/03/14	−589
1957/03/02	−255	1989/09/19	−255
1957/09/05	−324	1989/10/21	−267
1957/09/13	−427	1989/11/17	−266
1957/09/23	−303	1990/04/10	−281
1958/02/11	−426	1991/03/25	−298
1958/07/08	−330	1991/10/29*	−254
1958/09/04	−302	1991/11/09	−354
1958/07/15	−429	1992/05/10	−288
1960/04/01	−327	2000/04/07*	−288
1960/04/30	−325	2000/07/16*	−301
1960/10/07	−287	2001/03/31*	−387
1960/11/13	−339	2001/04/11*	−271
1961/10/28	−272	2001/11/06*	−292
1967/05/26	−387	2003/10/30*	−353
1970/03/08*	−284	2003/10/30*	−383
1981/04/13*	−311	2003/11/20*	−422
1982/07/14*	−325	2004/11/08*	−373
1982/09/06*	−289	2004/11/10*	−289
1986/02/09	−307	2005/05/15*	−263

Table 3 Average of peak values of *Dst* and of some interplanetary parameters associated with superstorms of the space era

Parameter	Average of peak values	Standard deviation	Median
Dst (nT)	324.3	67.3	302.0
V_{SW} (km/s)	799.1	160.6	743.0
B_{mag} (nT)	41.7	10.8	39.1
B_s (nT)	34.3	13.5	27.2
E_y (mV/m)	23.5	11.6	16.9
N_p (cm^{-3})	24.7	13.7	21.6
P_{dyn} (nPa)	25.7	14.8	21.3

Thus, in order to gain knowledge about extreme storms with larger peak intensities, one can try to look for them among historical extreme storms, as recorded only from ground observations, such as those studied by Tsurutani et al. (2003). Table 4 is a list of historical extreme storms (Table 1 of Tsurutani et al. 2003), for which the reported ΔH incursions at low geomagnetic latitude stations were < -500 nT.

Among the historical storms that occurred before 1957, as seen from Table 4, only the Carrington storm of September 2, 1859, has been extensively studied in terms of their solar origin and magnetospheric consequences (e.g. special issue of Advances of Space Research, edited by Clauer and Siscoe (2009)), due to the availability of solar and geomagnetic activity records. Such an extensive study was also motivated by the extremely large incursion of the ΔH component of the geomagnetic field, recorded at the Colaba/Bombay low latitude magnetic station (Tsurutani et al. 2003).

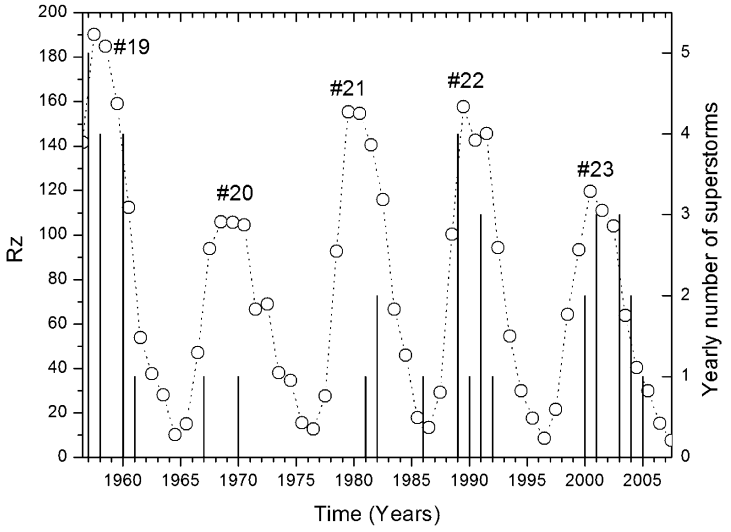

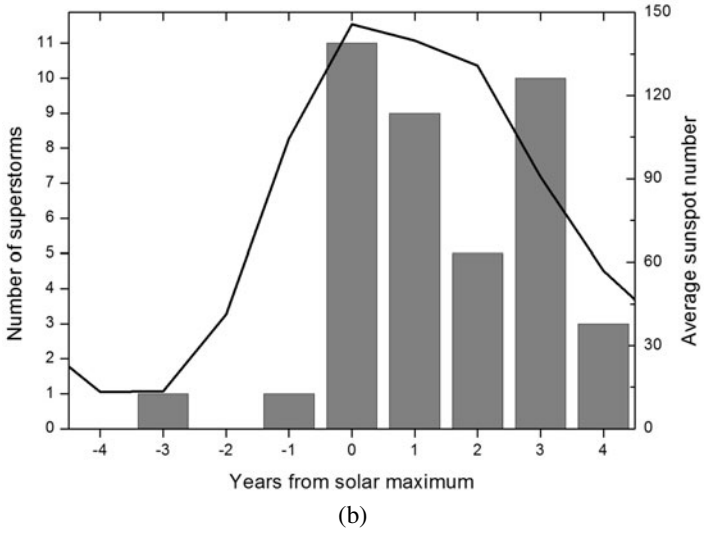

Fig. 5 (**a**) Solar sunspot cycle (*circles*) and distribution of the annual number of superstorms (*vertical bars*) since 1957. (**b**) Average solar cycle distribution for the superstorms shown in (**a**). (**c**) Seasonal distribution of the superstorms for the space era

The historical storms discussed by Tsurutani et al. (2003) and reproduced in Table 4 involve the "remarkable" storms since 1857, described by Ellis (1900), Moos (1910) and by Chapman and Bartels (1940). The Chapman and Bartels listing is reproduced in Table 1 with the addition of Bombay and Alibag–India, magnetometer data, as described by Tsurutani et al. (2003) and by Alex et al. (2006).

One can see in Table 4 that extreme historical storms have ΔH excursions of at least 450 nT, which is close to our defined extreme storm threshold for the *Dst* index (−400 nT). Since the historical storms had recorded ΔH values only at one low latitude station, we

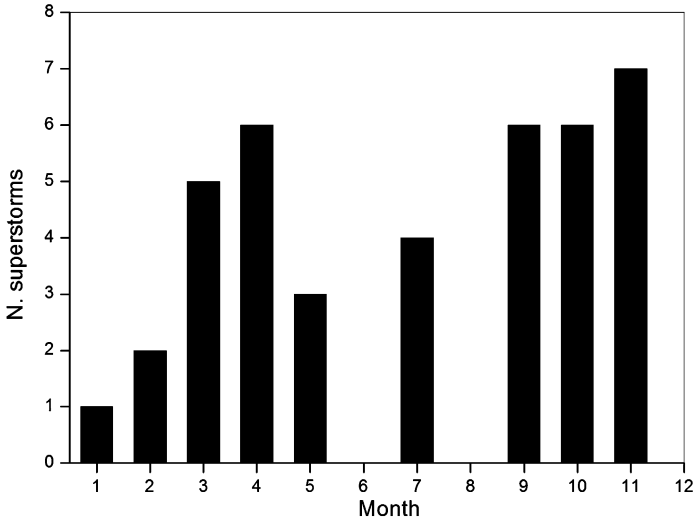

(c)

Fig. 5 (*Continued*)

can not make a direct comparison with the proper Dst index threshold. Nevertheless, as mentioned above, Echer and Gonzalez (2007) have shown that peak ΔH and peak Dst values are frequently comparable, at least for the range of superstorms and extreme storms studied during the space era.

4.1 The Carrington Storm

A very intense solar flare was observed by Carrington (1859) on September 1, 1859, a day before the extreme storm event. Many intense auroral events were observed on September 2, 1859 (Kimbal 1960) in association with the extreme ΔH incursion of approximately -1600 nT recorded at the Colaba/Bombay low latitude magnetic station.

With this information, Tsurutani et al. (2003) constructed a chain of associated processes/events in interplanetary space and in the magnetosphere after the intense solar flare observed by Carrington.

For that purpose, the authors used the following assumptions and information collected from the published literature:

- Travel time of 17.5 hours of the solar ejecta to the magnetosphere, as given by Carrington (1859).
- Function of solar wind speed at L1 in terms of the average ejecta/shock speed between the Sun and 1 AU, as studied by Cliver et al. (1990).
- Estimate of peak IMF intensity in terms of peak solar wind speed for ICMEs, as studied by Gonzalez et al. (1998).
- Estimate of peak value of the B_s component of the IMF for intense ICMEs, as studied by Gonzalez et al. (2004).
- Estimate of the reconnection/convection electric field, using studies about the efficiency of solar wind-magnetosphere coupling functions (Gonzalez et al. 1989).
- Observation of a very fast recovery of the large ΔH incursion, as measured by the Colaba/Bombay magnetometer (Tsurutani et al. 2003).

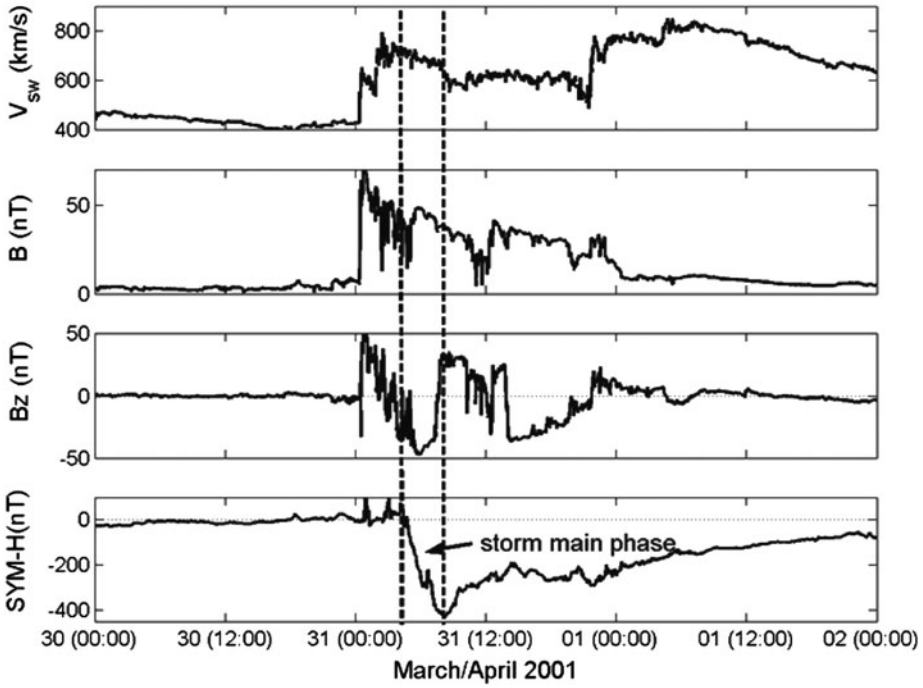

Fig. 6 Super intense storm of March 31, 2001, probably associated with a complex interplanetary cause involving at least two interacting clouds. The storm main phase (marked by *dotted lines*) was apparently influenced (compressed) by the second cloud

– Observations of auroras recorded at very low latitudes (Kimbal 1960).

Figure 8 summarizes the main results of the Tsurutani et al. (2003) study. A convection electric field of about 20 mV/m, obtained through the chain of processes listed on this figure, was used to study the ring current intensification and the inner magnetospheric dynamics related with the ring current and plasmapause positions. These values are in a good agreement with the latitudinal positions of the low latitude auroras observed during that event. These ring current and plasmapause positions were estimated by Tsurutani et al. (2003) from cold and hot plasma population limits obtained from a general expression for the inner magnetospheric electric potential, once the convection electric field was determined.

The estimated peak Dst value of about -1160 nT (Gonzalez et al. 2010) is in a fairly good agreement with the measured peak "Dst" value of -1050 nT, obtained when the reported 15 min average values of ΔH from the Colaba magnetometer were averaged for one hour, as it is usually done for the Dst index (although, of course, one is still dealing with the limitation of having only one low latitude station).

4.2 The 1972 Storm

Vaisberg and Zastenker (1976) determined the average speed of the August 1972 ejecta by measuring the time delay between the flare onset to the shock detection at 1 AU. Their average speed estimate was 2850 km/s, leading to a delay time of 14.6 hours, which is less than that for the Carrington storm. Thus, with the methodology described in the discussion of

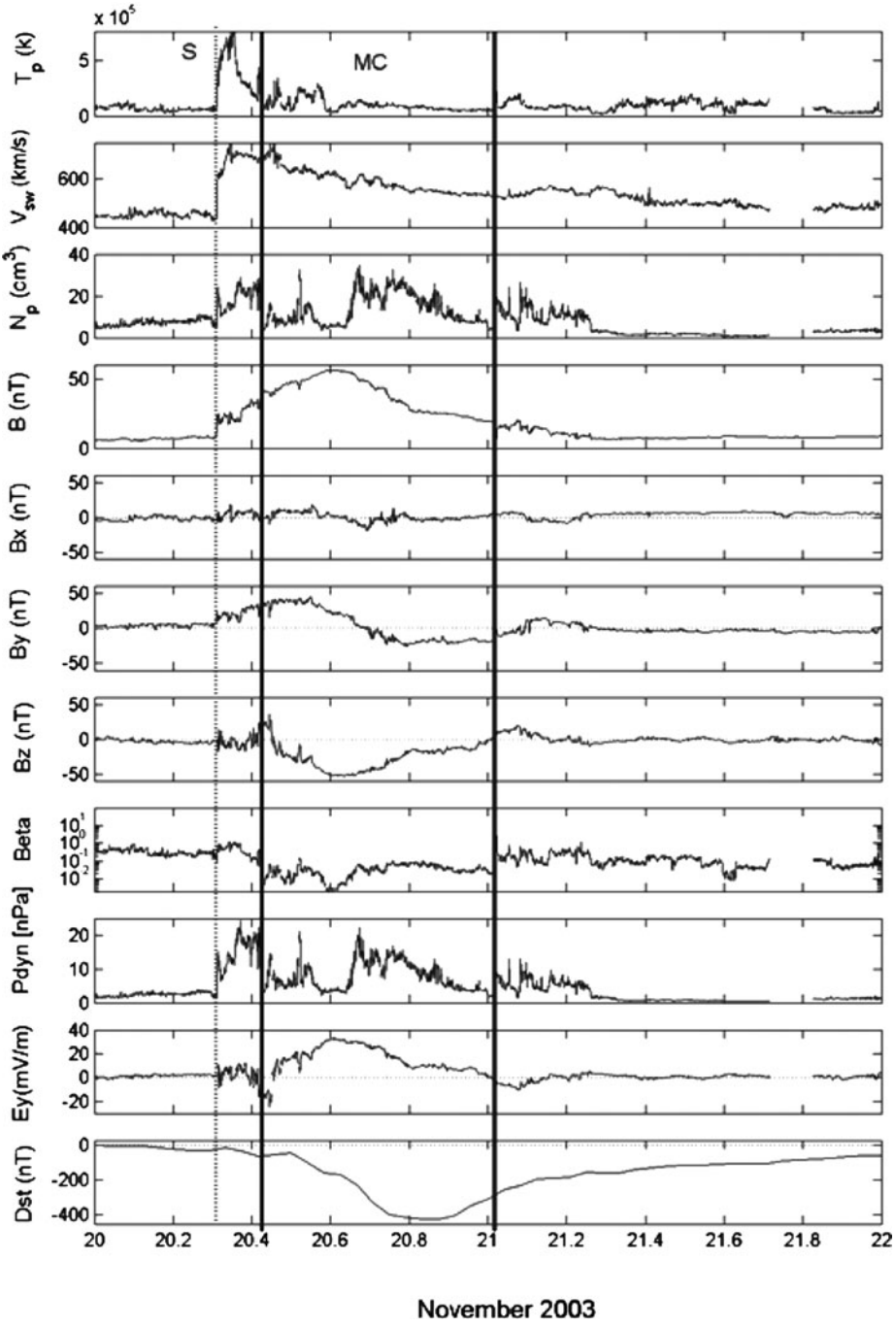

Fig. 7 *ACE* solar wind and *Dst* index for the largest geomagnetic storm of the solar cycle 23 $Dst_p = 422$ nT, 20 November 2003. Panels are solar wind proton temperature (T_p), solar wind speed (V_{sw}), proton density (N_p), magnetic field magnitude (B), and components (B_x, B_y, B_z) in GSM, plasma beta parameter (*Beta*), dynamic pressure (P_{dyn}), dawn-dusk electric field component (E_y), and *Dst* index

Table 4 Chronological list of extreme magnetic storms[a]

Storm	Year	Month	Day	H range[d] nT	Dst nT	Station	Geomagnetic[e] latitude N	Geomagnetic[e] longitude E
1	1859	September	1–2	1720		Bombay	9.87°	142.7°
		September	1–2	>700[b,c]		Kew	54.47°	82.5°
2	1859	October	12	980		Bombay	9.87°	142.7°
3	1872	February	4	1020		Bombay	9.87°	142.7°
4	1882	November	17	450		Bombay	9.87°	142.7°
		November	17	>1090[b,c]		Greenwich	54.40°	82.2°
5	1903	October	31	820		Bombay	9.87°	142.7
		October	31	>950[b,c]		Postdam	52.66°	96.2°
6	1909	September	25	>1500[b,c]		Postdam	52.66°	96.2°
7	1921	May	13–16	>700		Alibag	9.61°	142.7
		May	13–16	1060		Postdam	52.66°	96.2°
8	1928	July	7	780		Alibag	9.61°	142.7°
9	1938	April	16	530		Alibag	9.61°	142.7°
		April	16	1900[b]		Postdam	52.66°	96.2°
10	1957	September	13	580	−467	Alibag	9.61°	142.7°
11	1958	February	11	660	−426	Alibag	9.61°	142.7°
12	1989	March	13	640	−589	Kakioka	25.97°	205.1°

[a]The list includes the "Remarkable magnetic storms" described by Moos (1910) and Chapman and Bartels (1940)

[b]The values recorded at the mid-latitude stations could have an ionospheric component associated with the activity

[c]Saturation of the instrument

[d]H-range is defined as the difference between the maximum and the minimum value of H during the storm event

[e]Geomagnetic coordinates for all the observatories are computed for the year 1940 based on the IGRF model (courtesy NGDC site)

Fig. 8, one could estimate an associated reconnection/convection electric field of 25 mV/m for the 1972 event.

Unfortunately there was no IMF measurement for the 1972 storm near 1 AU, but Tsurutani et al. (1992b), examining in detail the Pioneer 10 data at ≈2 AU, observed that the magnetic cloud responsible for this event had its axis highly tilted from the ecliptic. Tsurutani et al. (2003) also suggested that the IMF intensity, extrapolated back to the Earth from its point of measurement by Pioneer 10, could have been as large as 80 nT or more.

Figure 9 shows the polarities of magnetic clouds with rotations (a) in the XZ plane, as regular geoeffective magnetic clouds usually have, and (b) in the XY plane, as it could have been the case for the 1972 event. Since the B_z field of the 1972 cloud was observed northward by Pioneer 10, the polarity of the cloud probably was as that depicted in Fig. 9 (counterclockwise). However, if the rotation of the cloud could have been in the opposite direction (clockwise), the associated B_z field would have been southward, which could have produced an extreme storm at Earth.

Thus, if the 1972 event would have involved an ICME with its axis on the ecliptic or a rotation of the cloud in the clockwise sense, the resulting storm at Earth would have been as intense as the Carrington event or perhaps even more (because the ejecta speed was larger).

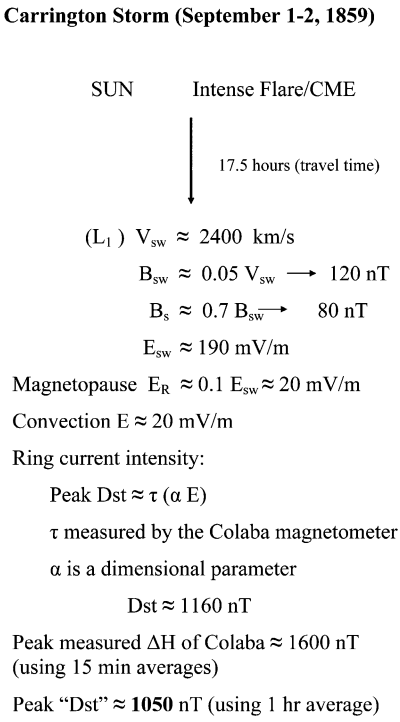

Fig. 8 Summary of the main results obtained by Tsurutani et al. (2003), using the assumptions and information published in the literature, as described in the text. The resulting magnetic fields are shown. The given magnitudes are peak values

4.3 Solar Activity Dependence of Extreme Storms

Figure 10 shows the space era extreme storm intensities plotted with the sunspot number against time. The recorded events occurred since solar cycle 9. Before that time there is little useful data due to the lack of reliable measurements. In this figure, the height of the vertical bars indicate the measured range of ΔH for the historical events, as listed on Table 4, or the measured peak Dst for the events of the space era.

From Fig. 10 one can observe the following:

- There is at least one extreme event for almost every solar cycle, with the exceptions of cycles 13 and 18. In 1958 there were 2 events (shown only as one event in this figure). From the 13 extreme events of this figure, 9 events occurred around solar maximum or at the early descending phase of the cycles, whereas 2 occurred during the ascending phase and 2 at the late descending phase of the cycles. None occurred at solar minimum.
- There is a tendency for the intensity of the events to have been larger for most of the historical events as compared with the intensity of the recent extreme events, although this apparent tendency could be related to the fact that we have plotted only the range of ΔH for the historical storms, whereas for the space era events the real Dst values were given.

Hoyt and Schatten (1997) have studied the Gleissberg solar modulation of the sunspot solar cycles, with a duration of 8 to 10 solar cycles between consecutive minima of the modulation. These authors place the last two Gleissberg minima centered approximately around 1900 and 2010, with the maxima centered approximately at 1840 and 1960. Hoyt and Schatten (1997) also indicate the occurrence of secondary Gleissberg maxima during

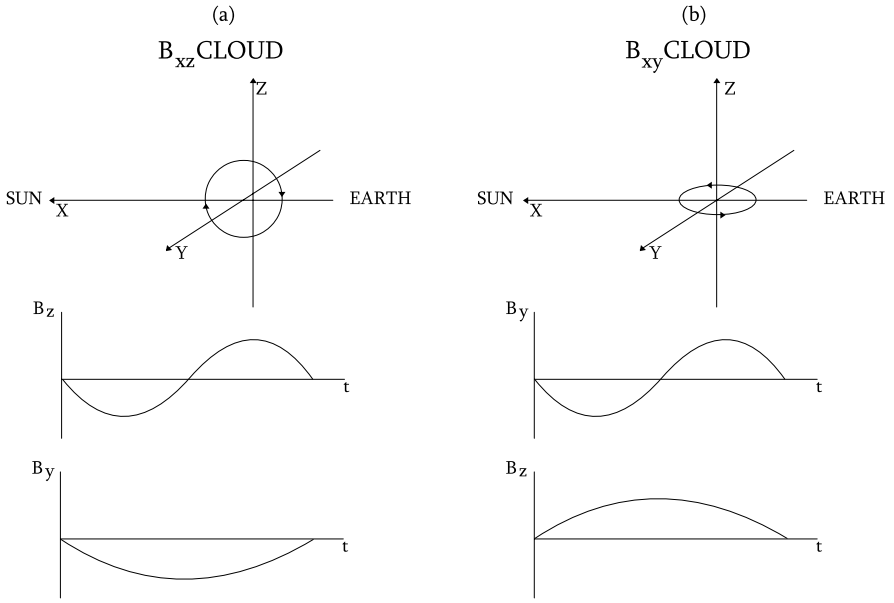

Fig. 9 Polarities of magnetic clouds, (**a**) for a cloud with a rotation in the X-Z plane, (**b**) for a cloud with a rotation (*counter clockwise*) in the X-Y plane

solar cycles # 11 and # 21 for the last two Gleissberg cycles. The dotted lines in Fig. 10 illustrate the two Gleissberg modulations.

The Carrington extreme storm occurred in cycle # 10, right before the cycle with the secondary maximum of the former Gleissberg cycle. It is interesting to note that the 1972 storm, which could have been as intense as the Carrington event, occurred on cycle # 20, also one cycle before that with the secondary maximum of the last Gleissberg cycle. Further, these cycles (# 10 and # 20) had similar peak amplitudes in their sunspot numbers (around 100), and two extreme storms with peak $\Delta H(Dst)$ values of ≤ -500 nT occurring during their previous cycles (# 9 and # 19).

5 Discussion

As shown in Table 1, the four main interplanetary structures that caused intense geomagnetic storms during solar cycle 23 were those that have been previously discussed in the literature (e.g. Tsurutani et al. 1995, 2006; Gonzalez et al. 1999) as being the most common sources of intense storms, although these authors presented their results only for separate phases (maximum or declining) of the solar cycle. Table 1 also shows that the two most common structures driving intense storms for the full solar cycle were magnetic clouds and sheath fields. These results are in agreement with those anticipated in the works by Gonzalez and Tsurutani (1987) and Tsurutani et al. (1988). One can see in Fig. 1 that the four dominant interplanetary structures driving intense storms during solar cycle 23 vary according to the phase of the cycle, being magnetic clouds, then sheath fields, and then sheath fields followed by a magnetic cloud for the rising phase; sheath fields, then sheath fields followed by a magnetic cloud and then magnetic clouds for the maximum phase; and magnetic clouds,

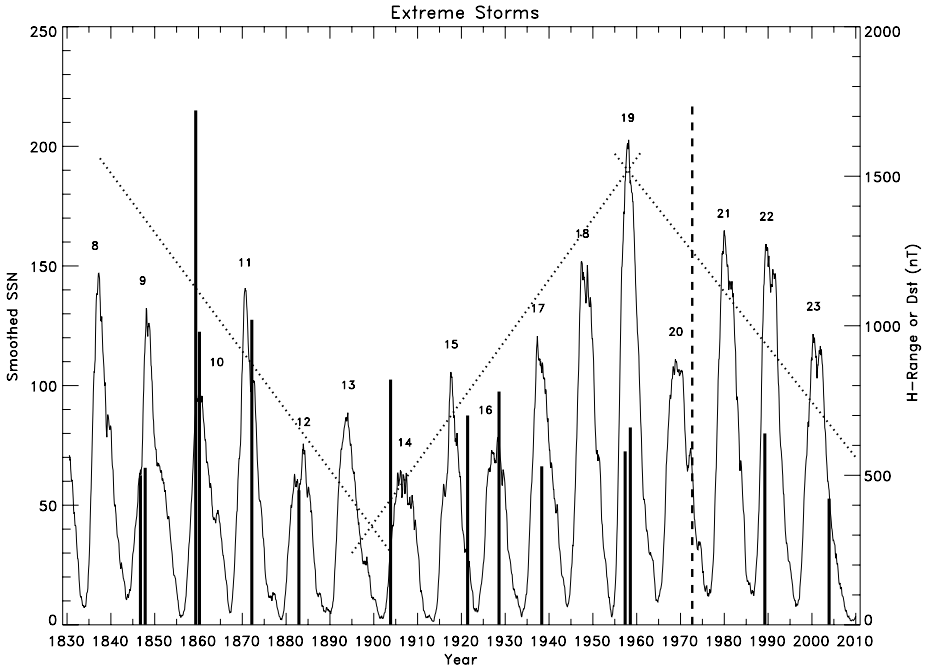

Fig. 10 Solar cycle distribution of the historical and space era extreme storms, with the bar heights indicating the observed ΔH or Dst intensity incursions. The *dotted lines* join the years of maximum and minimum of the last two Gleissberg cycles of solar activity. The *dashed vertical line* indicates the failed Carrington-type storm of August 1972

then CIRs and then sheath fields for the declining phase. Figure 1 also shows that magnetic clouds are the top dominant structures, both for the rising as for the declining phases, to drive intense storms, whereas sheath fields are the dominant structures during solar maximum. Since intense sheath fields are associated with intense shocks, this latter result is in agreement with the expected intensification of the occurrence of CMEs during solar maximum (e.g. Gonzalez et al. 1999). During the declining phase, another important and abundant interplanetary structure driving intense storms are CIRs, as expected from the larger presence of the associated high speed streams during this phase of the solar cycle (Tsurutani et al. 2006). However, such structures are less geoeffective, leading to storms with peak Dst values ≥ -150 nT. Figure 1 also shows that CIRs have only a minor contribution during the rising and maximum phases.

The yearly distribution of intense storms for solar cycle 23, as seen in the histograms of peak Dst values of Fig. 3, shows the expected dual-peak distribution (Gonzalez et al. 1990a), with the first peak appearing at solar maximum and the second peak in the early part of the declining phase. From the information obtained in Fig. 1, the first peak could be associated with sheath fields as the main driving structures, while magnetic clouds appear to be the main responsible structures for the second peak.

Echer et al. (2008a) have found that all intense storms studied for solar cycle 23 were caused by IMF B_s fields. Both linear correlation and multiple linear correlation showed much higher dependence of Dst on $B_s(E_y)$ than on other interplanetary parameters. These results indicate that the possibility that intense storms are caused by intense solar wind

pressure (shocks), high speed streams, or IMF B_y with B_z north conditions, is small or nonexistent. Thus, magnetic reconnection due to intense southward IMFs is the dominant mechanism (Gonzalez et al. 1994). Echer et al. (2008b) also tested the empirical interplanetary criteria of long duration ($\gtrsim$3 h) $B_s \gtrsim 10$ nT or $E_y \gtrsim 5$ mV/m, leading to intense storms (Gonzalez and Tsurutani 1987). They found that more than 70% of the studied storms satisfied these criteria.

For four out of the five extreme storms of the space era, we unfortunately can not study their associated geoeffective interplanetary structures because of lack of data. For the three events of 1957 and 1958 there were no interplanetary monitors yet, and for the March 1989 event no solar wind data was recorded due to the strong saturation of the instruments. Only the extreme storm of November 2003 had solar wind data (Fig. 5b), showing a magnetic cloud as the interplanetary structure responsible for the storm development. Such a magnetic cloud had its axis normal to the ecliptic, as in the 1972 event, with the polarity of the cloud having a clockwise rotation, thus producing an intense southward B_z field, opposite to what occurred in the 1972 event. This reinforces the considerations made above about the 1972 event, as being a failed Carrington-type storm. In the November 2003 event the cloud speed had peak values of only 800 km/s, whereas the 1972 cloud speed attained values of $\approx$2800 km/s. Considering the B–V relationship studied by Gonzalez et al. (1998) for magnetic clouds, this difference in the cloud speeds between the 2003 and the 1972 extreme storms could imply in a peak Dst storm of ≈ -1400 nT for the 1972 event, since the storm of 2003 reached a peak Dst value of only -400 nT. Thus, if the magnetic cloud of the 1972 event would have carried a polarity with a clockwise rotation, the ensuing extreme storm could have been even more intense than the Carrington storm (that apparently reached a peak Dst value of only -1100 nT).

The solar and seasonal distributions of superintense storms displayed in Figs. 5b and 5c show similar results as those obtained before for intense storms, namely that they have a dual-type distribution in the solar cycle, one at solar maximum and the second at the descending phase of the cycle (Gonzalez et al. 1990a), and a seasonal distribution showing the equinoctial peaks and an additional peak in July (Clúa de Gonzalez et al. 2001).

The average peak values of the solar wind parameters involved in the superintense storms, as shown in Table 3, indicate the presence of fairly large values of the solar wind speed, density and dynamic pressure, of the IMF intensity and of the B_s field. These large values certainly indicate that the reconnection process at the magnetopause also becomes very intense, leading into large values of the convection electric field and of the consequent large energization of the ring current (Gonzalez et al. 1994). Intensities of the ring current (Dst) as large as -1000 nT, as in the Carrington event, can be expected from theory (Vasyliunas 2010). Also, the ring current intensity does not seem to saturate with large values of the solar wind parameters (speed and B_s), although the polar cap electric potential seems to do so (e.g. Hairston et al. 2003, 2005; Shepherd et al. 2002; Lopez et al. 2009).

From the considerations made on the 1972 intense storm, we learn that magnetic clouds accompanying very fast ejecta can lead to the occurrence of extreme events depending on the polarity of the cloud. If the axis of the cloud is in the ecliptic the chances to have an extreme storm are large, whereas if the axis is more transverse to the ecliptic, as in the 1972 case, an extreme event can be expected only when the polarity of rotation of the cloud is such that a large B_s field is produced. For the 1972 case, the polarity was counter-clockwise, thus producing a large northward B_z field. If the polarity would have been clockwise, a large southward B_z field could have existed, thus leading to the development of an extreme storm. This polarity may depend on some solar cycle features that are worth investigating.

For clouds with the axis on the ecliptic, such a polarity could depend on the polar magnetic polarity of the Sun which alternate from cycle to cycle. For these the difference in polarity only leads to a different sequence of north-south B_z, or south-north B_z in the approaching cloud, leading to some differences in the magnetospheric response and in the intensity of the developing storm (Gonzalez et al. 1990b).

If the 1972 event would have involved a magnetic cloud with an appropriate polarity, the consequential storm would have been an extreme event, with an intensity as large as that of the Carrington storm or perhaps even larger. We were lucky, since the ground electric technology present in 1972 was certainly much more vulnerable than that of 1859. It is known that in 1859, the very intense ionospheric currents at middle latitudes produced very intense geomagnetic induction currents that burned many telegraph systems in Europe and in the US (e.g. Loomis 1891; Kappenman 2006). The dashed vertical line in Fig. 10 indicates the failed Carrington-type storm of August 1972.

If the considerations mentioned in Sect. 4 with respect to the possible occurrence of Carrington-type storms is reasonable, by comparing the time of occurrence of the Carrington storm and of the failed extreme storm of 1972 with respect to the Gleissberg cycle of solar activity, one could suggest that extreme events of that intensity can be expected to occur once in a century, with a tendency to appear before and close to the secondary maximum of the descending phase of the Gleissberg cycle. Thus, according to this reasoning, and since we are presently at a minimum of a Gleissberg cycle, we may still be at nearly six solar cycles distant from the next possible Carrington-type storm.

One final comment refers to the abnormally extended minimum of the last solar cycle. From Fig. 10 one can notice that this minimum coincides with a Gleissberg minimum (Hoyt and Schatten 1997). This combination could explain in part this abnormality and also the probable low peak sunspot number expected for coming years.

Acknowledgements W.D.G. would like to thank the "Fundação de Amparo à Pesquisa do Estado de São Paulo", FAPESP (2008/06650-9) and the "Conselho Nacional de Pesquisas", CNPq (PQ-300321/2005-8). E.E. would like to thank the FAPESP (2007/52533-1) and CNPq (PQ-300211/2008-2) and A.L.C.G. would like to thank CNPq (PQ-342734/2008-2). Portions of this work were done at the Jet Propulsion Laboratory, California Institute of Technology under contract with NASA.

References

S. Alex, S. Mukherjee, G.S. Lakhina, Geomagnetic signatures during the intense geomagnetic storms of October 29 and November 20, 2003. J. Atmos. Sol.-Terr. Phys. **68**, 769 (2006)

M.V. Alves, E. Echer, W.D. Gonzalez, Geoeffectiveness of corotating interaction regions as measured by *Dst* index. J. Geophys. Res. **111**, 1–10 (2006). doi:10.1029/2005JA011379

A. Balogh, V. Bothmer, N.U. Crooker, R.J. Forsyth, G. Gloeckler, A. Hewish, M. Hilchenbach, R. Kallenbach, B. Klecker, J.A. Linker, E. Lucek, G. Mann, E. Marsch, A. Posner, I.G. Richardson, J. Schmidt, M. Scholer, Y.M. Wang, R.F. Wimmer-Schweingruber, M.R. Aellig, P. Bochsler, S. Hefti, Z. Mikic, The solar origin of corotating interaction regions and their formation in the inner heliosphere. Space Sci. Rev. **89**(1–2), 142–178 (1999). doi:10.1023/A:1005245306874

L.F. Burlaga, K.W. Behannon, L.W. Klein, Compound streams, magnetic clouds, and major geomagnetic storms. J. Geophys. Res. **92**(A6), 5725–5734 (1987)

R.C. Carrington, Description of a singular appearance seen in the Sun on September. Mon. Not. R. Astron. Soc. **XX**(13), 13–15 (1859)

S. Chapman, J. Bartels, *Geomagnetism* (Oxford University Press, London, 1940)

C. Cid, E. Saiz, Y. Cerrato, Comment on 'Interplanetary conditions leading to superintense geomagnetic storms ($Dst \leq -250$ nT) during solar cycle 23' by E. Echer et al. Geophys. Res. Lett. **35**, 1–3 (2008). L21107, doi:10.1029/2008GL034731

C.R. Clauer, G. Siscoe, The great historical geomagnetic storm of 1859: a modern look. Adv. Space Res. **38**, 117–118 (2009). Especial issue

E.W. Cliver, J. Feynmann, H.B. Garret, An estimate of the maximum speed of the solar wind, 1938–1989. J. Geophys. Res. **95**, 17103 (1990)
A.L. Clúa de Gonzalez, V.M. Silbergleit, W.D. Gonzalez, B.T. Tsurutani, Annual variation of geomagnetic activity. J. Atmos. Sol.-Terr. Phys. **63**, 367–374 (2001)
A. Dal Lago, L.E.A. Vieira, E. Echer, W.D. Gonzalez, A.L. Clúa de Gonzalez, F.L. Guarnieri, L. Balmaceda, J.C. Santos, M.R. da Silva, A. De Lucas, N.J. Schuch, Great geomagnetic storms in the rise and maximum of solar cycle 23. Braz. J. Phys. **34**, 1542 (2004)
E. Echer, W.D. Gonzalez, Geoeffectiveness of interplanetary shocks, magnetic clouds, sector boundary crossings and their combined occurrence. Geophys. Res. Lett. **31**(1–4), L09808 (2004). doi:10.1029/2003GL019199
E. Echer, W.D. Gonzalez, Ring current asymmetry during superintense magnetic storms, in *Proceedings of the 10th International Congress, Braz* (Geophys. Soc. Rio de Janeiro, Rio de Janeiro, 2007)
E. Echer, V.M. Alves, W.D. Gonzalez, A statistical study of magnetic cloud parameters and geoeffectiveness. J. Atmos. Sol.-Terr. Phys. **67**, 839–852 (2005)
E. Echer, W.D. Gonzalez, B.T. Tsurutani, Interplanetary conditions leading to superintense geomagnetic storms ($Dst \leq -250$ nT) during solar cycle 23 (1996–2006). Geophys. Res. Lett. **35**(1–5), L06S03 (2008a). doi:10.1029/2007GL031755
E. Echer, W.D. Gonzalez, B.T. Tsurutani, A.L. Clúa de Gonzalez, Interplanetary conditions causing intense geomagnetic storms ($Dst \leq -100$ nT) during solar cycle 23 (1996–2006). J. Geophys. Res. **113**(1–6), A05221 (2008b). doi:10.1029/2007JA012744
W. Ellis, The relation between magnetic disturbance and sunspot frequency. Mon. Not. R. Astron. Soc. **60**, 142 (1900)
W.D. Gonzalez, F.S. Mozer, A quantitative model for the potential resulting from reconnection with an arbitrary interplanetary magnetic field. J. Geophys. Res. **79**(28), 4186–4194 (1974)
W.D. Gonzalez, B.T. Tsurutani, Criteria of interplanetary parameters causing intense magnetic storms ($Dst \leq -100$ nT). Planet. Space Sci. **35**, 1101–1109 (1987)
W.D. Gonzalez, B.T. Tsurutani, A.L. Clúa de Gonzalez, E.J. Smith, F. Tang, S.I. Akasofu, Solar wind-magnetosphere coupling during intense magnetic storms. J. Geophys. Res. **94**, 8835 (1989)
W.D. Gonzalez, A.L. Clúa de Gonzalez, B.T. Tsurutani, Dual-peak solar cycle distribution of intense geomagnetic storms. Planet. Space Sci. **38**, 181–187 (1990a)
W.D. Gonzalez, B.T. Tsurutani, L. Lee, Comment on the polarity of magnetic clouds. J. Geophys. Res. **95**, 17267 (1990b)
W.D. Gonzalez, J.A. Joselyn, Y. Kamide, H.W. Kroehl, G. Rostoker, B.T. Tsurutani, V.M. Vasyliunas, What is a geomagnetic storm? J. Geophys. Res. **99**(A4), 5771–5792 (1994)
W.D. Gonzalez, A.L. Clúa de Gonzalez, A. Dal Lago, B.T. Tsurutani, J.K. Arballo, G.S. Lakhina, B. Buti, C.M. Ho, S.T. Wu, Magnetic cloud field intensities and solar wind velocities. Geophys. Res. Lett. **25**, 963 (1998)
W.D. Gonzalez, B.T. Tsurutani, A.L. Clúa de Gonzalez, Interplanetary origin of magnetic storms. Space Sci. Rev. **88**, 529–562 (1999)
W.D. Gonzalez, B.T. Tsurutani, R.P. Lepping, R. Schwenn, Interplanetary phenomena associated with very intense geomagnetic storm. J. Atmos. Sol.-Terr. Phys. **64**, 173–181 (2002)
W.D. Gonzalez, A.L. Clúa de Gonzalez, L.E.A. Vieira, B.T. Tsurutani, Prediction of peak Dst from CME/magnetic cloud-speed observations. J. Atmos. Sol.-Terr. Phys. **66**, 161 (2004)
W.D. Gonzalez, E. Echer, A.L. Clúa de Conzalez, B.T. Tsurutani, Interplanetary origin of intense geomagnetic storms ($Dst \leq -100$ nT) during solar cycle 23. Geophys. Res. Lett. **34**(1–4), L06101 (2007). doi:10.1029/2006GL028879
W.D. Gonzalez, E. Echer, A.L. Clúa de Gonzalez, B.T. Tsurutani, Reply to 'Comment by Y.I. Yermolaev and M.Y. Yermolaev on 'Interplanetary origin of intense geomagnetic storms ($Dst \leq -100$ nT) during solar cycle 23'. Geophys. Res. Lett. **35**(1–2), L01102 (2008). doi:10.1029/2007GL031856
W.D. Gonzalez, E. Echer, A.L. Clúa de Gonzalez, B.T. Tsurutani, G.S. Lakhina, Extreme geomagnetic storms, recent Gleissberg cycles and space era-superintense storms. J. Atmos. Sol.-Terr. Phys. (2010). doi:10.1016/j.jastp.2010.07.023. http://www.sciencedirect.com/science/article/B6VHB-50NBNXT-2/2/18a6e3a828df6058d7b7e66430f1d5b2
J.T. Gosling, D.J. McComas, J.L. Phillips, F. Tang, S.I. Akasofu, S.J. Bame, Geomagnetic activity associated with earth passage of interplanetary shock disturbances and coronal mass ejections. J. Geophys. Res. **96**(A5), 7831–7839 (1991)
M.R. Hairston, T.W. Hill, R.A. Heelis, Observed saturation of the ionospheric polar cap potential during the 31 March 2001 storm. Geophys. Res. Lett. **30**(6), 1325 (2003). doi:10.1029/2002GL015894
M.R. Hairston, K.A. Drake, R. Skoug, Saturation of the ionospheric polar cap potential during the October–November 2003 superstorms. J. Geophys. Res. **110**(1–12), A09S26 (2005). doi:10.1029/2004JA010864
D.V. Hoyt, K. Schatten, *The Role of the Sun in Climate Change* (Oxford University Press, London, 1997)

K.E.J. Huttunen, H.E.J. Koskinen, R. Schwenn, Variability of magnetospheric storms driven by different solar wind perturbations. J. Geophys. Res. **107**(A7), 1–8 (2002). doi:10.1029/2001JA900171

Y. Kamide, N. Yokoyama, W.D. Gonzalez, B.T. Tsurutani, I.A. Daglis, A. Brekke, S. Masuda, Two-step development of geomagnetic storms. J. Geophys. Res. **103**, 6917 (1998)

J.G. Kappenman, Great geomagnetic storms and impulsive geomagnetic field disturbance events—an analysis of observational evidence including the great storm of May 1921. Adv. Space Res. **38**, 188 (2006)

D.S. Kimbal, A study of the Aurora of 1859, Sci. Rept., UAG-R 109, University of Alaska, Fairbanks, Alaska, 1960

G.S. Lakhina, S. Alex, B.T. Tsrutani, W.D. Gonzalez, *Research on Historical Records of Geomagnetic Storms*, Coronal and Stellar Mass Ejections (Cambridge University Press, Cambridge, 2005), 226 pp.

E. Loomis, On the great auroral exhibition of Aug. 28th to Sept. 4, 1859, and on Auroras generally. Am. J. Sci. **82**, 318 (1891)

R.E. Lopez, J.G. Lyon, E. Mitchell, R. Bruntz, V.G. Merkin, S. Brogl, F. Tofolletto, M. Wiltberger, Why doesn't the ring current injection rate saturate? J. Geophys. Res. **114**, 1–8 (2009). doi:10.1029/2008JA013141

N.A.F. Moos, *Magnetic Observations Made at the Government Observatory*, Bombay 1846–1905, Part II, Gov. Centr. Press, Bombay, 1910

I.G. Richardson, D.F. Webb, D.B. Berdichevsky, D.A. Biesecker, J.C. Kasper, R. Kataoka, J.T. Steinberg, B.J. Thompsom, C.C. Wu, A.N. Zhukov, Major geomagnetic storms ($Dst \leq -100$ nT), generated by corotating interaction regions. J. Geophys. Res. **111**(1–7), A07S09 (2006). doi:10.1029/2005JA011476

S.G. Shepherd, R.A. Greenwald, J.M. Ruohoniemi, Cross polar cap potentials measured with super dual auroral radar network during quasi-steady solar wind and interplanetary magnetic field conditions. J. Geophys. Res. **107**(A7), 1094 (2002). doi:10.1029/2001JA000152

N. Srivastava, Predicting the occurrence of superstorms. Ann. Geophys. **23**, 2989 (2005)

B.T. Tsurutani, W.D. Gonzalez, Y. Kamide, F. Tang, S.I. Akasofu, E.J. Smith, Origin of interplanetary southward magnetic fields responsible for major magnetic storms near solar maximum (1978–1979). J. Geophys. Res. **93**, 8519–8531 (1988)

B.T. Tsurutani, W.D. Gonzalez, F. Tang, Y.T. Lee, Great magnetic storms. Geophys. Res. Lett. **19**, 73 (1992a)

B.T. Tsurutani, W.D. Gonzalez, F. Tang, Y.T. Lee, M. Okada, D. Park, Solar wind ram pressure corrections and an estimation of the efficiency of viscous interaction. Geophys. Res. Lett. **19**, 1993 (1992b)

B.T. Tsurutani, W.D. Gonzalez, A.L. Clúa de Gonzalez, F. Tang, J.K. Arballo, M. Okada, Interplanetary origin of geomagnetic activity in the declining phase of the solar cycle. J. Geophys. Res. **100**(A11), 21717–21733 (1995)

B.T. Tsurutani, W.D. Gonzalez, G.S. Lakhina, S. Alex, The extreme magnetic storm of 1–2 September 1859. J. Geophys. Res. **108**(1–8), 1268 (2003). doi:10.1029/2002JA009504

B.T. Tsurutani, L.F. Guarnieri, T. Fuller-Rowell, A.J. Manucci, W.D. Gonzalez, D.L. Judge, P. Gangopadhyay, A. Saito, T. Tsuda, O.P. Verkhoglyadova, G.A. Zambon, Extreme solar EUV flares and ICMEs and resultant extreme ionospheric effects: comparison of the halloween 2003 and the Bastille Day events. Radio Sci. **41**(1–7), RS5S07 (2006). doi:10.1029/2005RS003331

B.T. Tsurutani, E. Echer, L.F. Guarnieri, J.U. Kozyra, Cawses November 7–8, 2004, superstorm: complex solar and interplanetary features in the post-solar maximum phase. Geophys. Res. Lett. **35**(1–6), L06S05 (2008). doi:10.1029/2007GL031473

O.L. Vaisberg, G.N. Zastenker, Solar wind and magnetosheath observations at Earth during August 1972. Space Sci. Rev. **19**, 687 (1976)

V.M. Vasyliunas, The largest imaginable magnetic storm. J. Atmos. Sol.-Terr. Phys. (2010, in press). doi:10.1016/j.jastp.2010.05.012

Y.I. Yermolaev, M.Y. Yermolaev, Comment on 'Interplanetary origin of intense geomagnetic storms ($Dst \leq -100$ nT) during solar cycle 23' by W.D. Gonzalez et al. J. Geophys. Res. **35**(1–2), L01101 (2008). doi:10.1029/2007GL030281

J.C. Zhang, M.W. Liemohn, J.U. Kozyra, M.F. Thomsem, H.A. Elliot, J.M. Weygand, A statistical comparison of solar wind sources of moderate and intense geomagnetic storms at solar minimum and maximum. J. Geophys. Res. **111**(1–16), A01104 (2006). doi:10.1029/2005JA011065

J.C. Zhang, I.G. Richardson, D.F. Webb, N. Gopalswamy, E. Huttunen, J.C. Kasper, N.V. Nitta, W. Poomvises, B.J. Thompsom, C.C. Wu, S. Yashiro, A.N. Zhukov, Solar and interplanetary sources of major geomagnetic storms ($Dst \leq -100$ nT) during 1996–2005. J. Geophys. Res. **112**(1–19), A10102 (2007). doi:10.1029/2007JA012321